



Cite this: *Chem. Sci.*, 2022, **13**, 10939

All publication charges for this article have been paid for by the Royal Society of Chemistry

Received 16th July 2022
Accepted 30th August 2022

DOI: 10.1039/d2sc0397j
rsc.li/chemical-science

Introduction

To date, the stereoselective polymerization of substituted epoxides such as propylene oxide (PO) has remained an exclusive domain of relatively few metal-based polymerization systems.¹ First described in the early 1950s in the form of a heterogeneous FeCl_3 setup (Pruitt–Baggett catalyst) to deliver fractions of isotactic (*it*)-PPO,² later examples also include Al- and Zn-based compounds³ (*i.e.*, the Vandenberg catalyst^{4,5}).

A further significant breakthrough occurred in 2005–2008 when Coates and co-workers published their findings on (bimetallic) $\text{Co}(\text{III})$ catalysts.^{6,7} Conversion of *rac*-PO and many other epoxides was observed, resulting in excellent selectivity and high molar masses. The obtained *it*-polyethers were found to be semi-crystalline with sometimes surprisingly high melting points.⁸ Bimetallic ring-opening and an optimized Co–Co distance, embedded in a chiral environment, were reported to be essential.⁹ The Coates system is strictly enantioselective.

Despite these advances, to the best knowledge of the authors, there is currently no commercial epoxide polymerization process dedicated to deliver *it*- or *it*-enriched PPO or other aliphatic polyethers, with the exception of perhaps a single example.¹⁰ In view of the substantial amounts manufactured annually – PO is the second most important epoxide monomer after ethylene oxide – and the broad applicability of aliphatic polyethers,¹¹ there is certainly no lack of interest. Especially the

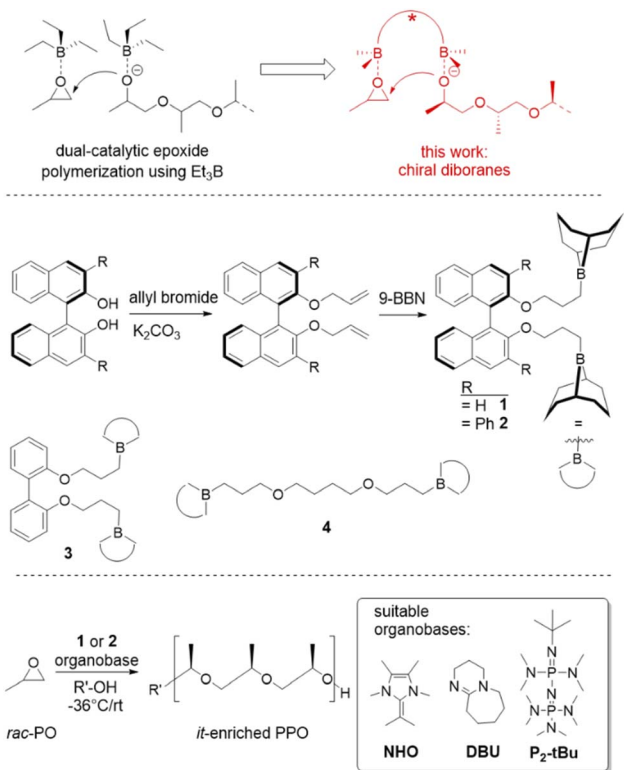
introduction of isotactic (enriched) polyether segments in more complex polymer architectures (*i.e.*, multiblocks containing also polyester sequences) seems promising in this regard, potentially opening up a new frontier to tailor the properties of polyether-based additives, where fine-tuning for applications in drug-delivery, tissue-engineering, rheology control or hydrogel formation can be conceived.¹²

Such requirements suggest potential benefits in the use of organocatalytic polymerization catalysts,^{13–16} where the controlled conversion of substituted epoxides has experienced a step change in the last few years.^{17,18} Especially the rise of a simple borane co-catalyst (triethylborane, Et_3B)^{19,20} has enabled the preparation of very well-defined polyether sequences with short reaction times under mild conditions.^{21,22} This borane can be employed together with a range of organobases, including very simple nitrogen bases.²³ Intriguingly, elegant work by Zhao and Ling has demonstrated that with such a setup even poly(ester-ether) multiblock motifs can be constructed – excessive transesterification is avoided during growth of the polyether blocks.²⁴ What deserves particular attention is the proposed mechanism, which necessitates two equivalents of Et_3B per organobase, a stoichiometry inherently linked to the simultaneous monomer activation and chain-end deactivation/coordination, which is also well-known from Lewis-pair polymerization (Scheme 1).²⁵ The viability of using multi-centered, onium-bridged (achiral) boranes for polymerization catalysis has been impressively demonstrated by Wu and others,^{26–28} while Du's work highlighted the potential of *in situ*-formed chiral boranes for, *i.e.*, asymmetric imine hydrogenation.^{29–31} Herein it will be shown that these characteristics can be exploited further to engender stereoselective polymerization

University of Stuttgart, Institute of Polymer Chemistry, 70569 Stuttgart, Germany.
E-mail: stefan.naumann@ipoc.uni-stuttgart.de

† Electronic supplementary information (ESI) available. CCDC 2168081. For ESI and crystallographic data in CIF or other electronic format see <https://doi.org/10.1039/d2sc0397j>





Scheme 1 Research rationale (top), diborane synthesis (middle) and polymerization setup (bottom) for the preparation of *it*-enriched PPO.

of *rac*-PO and other epoxides by using simple, chiral diboranes as co-catalysts, notably retaining the benefits of a well-controlled polymerization and a useful tolerance towards polyester-type initiators.

Results and discussion

In a first step, a strategy was developed to connect two borane functionalities to a chiral and well-available backbone. To this end, enantiopure (*R*)-BINOL (1,1'-bi-2-naphthol) and derivatives were first subjected to a Williamson etherification followed by hydroboration with 9-BBN (Scheme 1). This user-friendly two-step route delivered catalysts 1 and 2; crystal structure analysis confirmed expectations (Fig. 1). Analogously, control

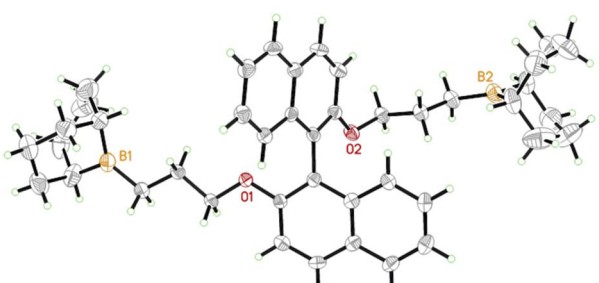


Fig. 1 Single crystal X-ray structure of chiral diborane 1. Naphthyl-naphthyl dihedral angle = 114°. See ESI and CCDC file 2168081.[†]

compounds 3 (biphenol-based) and 4 (linear aliphatic) were received.

A series of experiments was conducted, using 1 in combination with a range of organobases (including a specific *N*-heterocyclic olefin (NHO),^{32,33} a phosphazene and simple DBU, Scheme 1) and benzyl alcohol as initiator (Table 1). As a catalyst (Cat)/base (B) molar ratio a stoichiometry of at least 2 : 1 was chosen to ensure an excess of borane functionalities over propagating chain-ends. This was thought to enable monomer activation in spatial proximity to the growing polymeric species (Scheme 1, top) in a potentially stereoselective environment.

These initial experiments, conducted in the bulk (entries 1–6), indicated high conversion and a rapid increase in viscosity alongside a unimodal, narrow molar mass distribution. Accordingly, MALDI-ToF MS analyses underlined full control over the BnOH-derived end groups (Fig. 2) and thus excellent end group fidelity. Allyl-type termination, undesired and frequently observed in conventional PO polymerization as a result of transfer reactions,¹¹ was absent according to mass spectrometry and ¹H NMR spectroscopy studies, rendering this approach also suitable for constructing more complex polymer architectures (see below). Conversion and determined molar masses correlate linearly, as expected (Fig. S13[†]).

The observed degree of isotacticity in these first experiments, however, was only moderate. As determined *via* ¹³C NMR analyses, the proportion of isotactic diad placement (*m*) was found to be 62–69%, almost independent of the reaction temperature (−78 °C to 50 °C) and type of organobase. However, a reduction of [Cat]₀ by application of solvent pushed *m* up to > 80% (entry 7), indicating that bimolecular interaction between diboranes may be detrimental.²⁹ Even at very high PO loading (10 000 eq.) the polymerization runs to > 50% conversion and >120 000 g mol^{−1} (*M_n*) within 24 h (entry 8).

Kinetic studies using enantiopure PO revealed the (*S*)-PO to be the clearly preferred enantiomer for catalyst 1 (Fig. 2 and S14[†]). Notably this preference cleanly reverses when the (*S*)-enantiomer of 1 is employed, where a faster consumption of (*R*)-PO is observed (Fig. S16[†]). Zero order in monomer conversion was found, especially in the early stages of polymerization, which is in accordance with the particular characteristics of Lewis pair polymerizations using achiral diboranes (constant concentration of activated (borane-coordinated) monomer).^{25,26} Deviations from linear behavior can possibly be attributed to increasing viscosity (or even solidification) of the reaction mixture at higher conversions. Nonetheless, from these data the selectivity factor *s* can be approximated as the *k_s/k_r* ratio. For example, *s* = 8 for bulk polymerization at room temperature (Fig. S14[†]) improves to *s* = 16 under dilution (2 M in THF, Fig. 2). These findings nicely mirror the selectivity determined by ¹³C NMR under these conditions (Table 1) and also underline the positive impact of dilution on selectivity. To put this into perspective, a perfectly isoselective setup can be expected to deliver *s* > 100.⁸ ¹H NMR experiments, comparing the position of the PO monomer signal to that found in the presence of diborane, revealed no observable shift of the monomer or catalyst signals (Fig. S22[†]). This is in agreement with previous observations targeting Et₃B and indicates a relatively weak



Table 1 PO polymerization results using diborane (Cat)/organobase (B) setups, *BnOH* as initiator

#	Cat	B	B/Cat/BnOH/PO ^a	Solvent [PO]	T [°C]	t [h]	M _n ^b (calc.) [g mol ⁻¹]	D _M ^c	m ^d [%]	Conversion ^b [%]
1	1	NHO	1 : 2 : 5 : 2000	Bulk	50	3.0	9000	1.11	68	40
2	1	NHO	1 : 2 : 5 : 2000	Bulk	25	1.5	13 000	1.18	62	53
3	1	NHO	1 : 2 : 5 : 2000	Bulk	-36	2.0	16 000	1.18	65	70
4	1	NHO	1 : 2 : 5 : 2000	Bulk	-78	3.0	15 000	1.17	66	59
5	1	P₂-tBu	1 : 2 : 5 : 2000	Bulk	25	2.0	12 000	1.24	69	49
6	1	DBU	1 : 2 : 5 : 2000	Bulk	25	24	6000	1.18	62	27
7	1	NHO	1 : 2 : 2.5 : 1000	Toluene [2 M]	-36	24	25 000	1.14	82	80
8	1	NHO	1 : 2 : 2.5 : 10 000	Toluene [2 M]	-36	24	123 000	1.18	79	63
9	2	NHO	1 : 4 : 5 : 1000	Bulk	-36	24	5000	1.17	74	22
10	2	NHO	1 : 4 : 5 : 10 000	Bulk	-36	24	8000	1.11	80	7
11	2	NHO	1 : 2 : 2.5 : 1000	THF [4 M]	25	24	16 000	1.25	78	70
12	2	NHO	1 : 2 : 2.5 : 1000	THF [2 M]	25	8 d	4000	1.14	88	16
13	3	DBU	1 : 4 : 5 : 2000	Bulk	25	0.5	15 000	1.06	56	65
14	4	DBU	1 : 4 : 5 : 2000	Bulk	25	24	12 000	1.18	57	52

^a Molar ratio. ^b Determined via ¹H NMR. ^c Determined via GPC (CHCl₃). ^d Determined via ¹³C NMR.

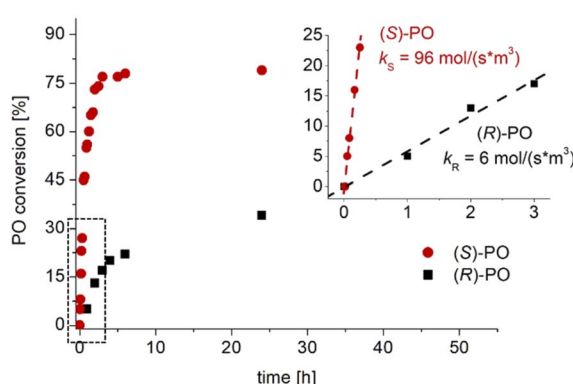
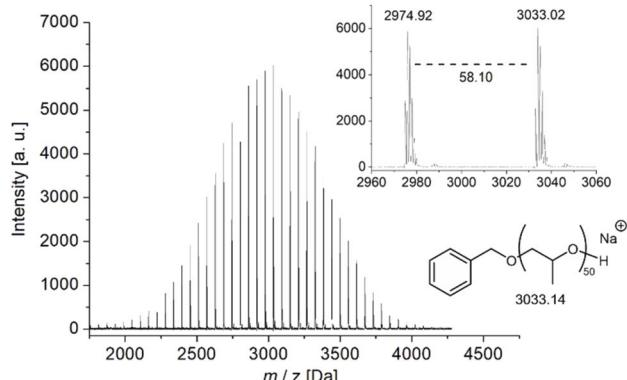
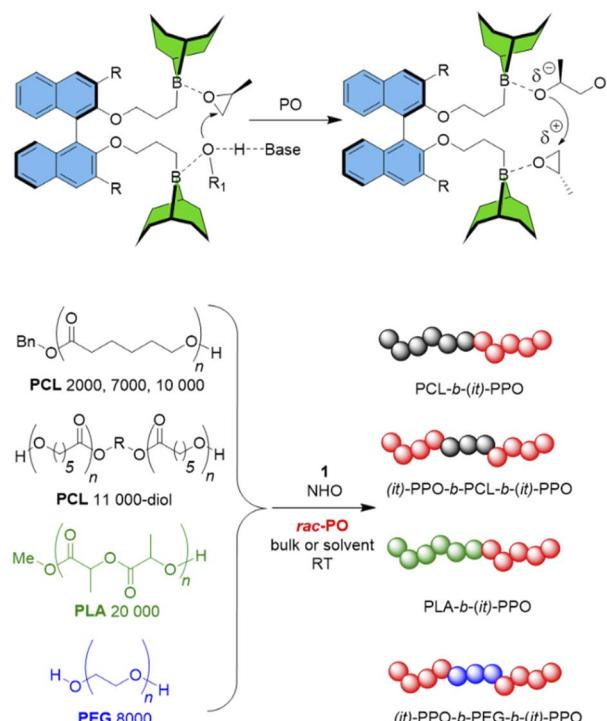


Fig. 2 Top: MALDI-ToF MS analysis of PPO prepared by the action of DBU/1 (bulk, -36 °C) with *BnOH* as initiator. Bottom: Polymerization kinetics using enantiopure monomer (2 M in THF, ambient, NHO/1/*BnOH*/PO = 1 : 2 : 5 : 2000 molar ratio).

monomer activation, potentially also supporting alternative polymerization models.²⁴ In any case, the monomer activation/chain-end deactivation mechanism (Schemes 1 and 2) must be considered as simplified and certainly requires further investigation.

Next, a (*R*)-BINOL-backbone carrying phenyl groups *ortho* to the hydroxyl functionalities was employed, aiming for a more efficient transfer of stereoinformation. Gratifyingly, application of diborane 2 entailed a further increase in selectivity. In the bulk, *m* was found to be 74–80%, while under dilute conditions an isotactic diad placement of *m* = 88% was observed. Molar mass distributions remained well-controlled (1.1 < D_M < 1.3), even up to relatively high molar masses (M_n > 40 000 g mol⁻¹). Compared to 1, this higher selectivity is accompanied by



Scheme 2 Top: Simplified cooperative mechanism in the presence of diborane, organobase, PO and initiator/propagating chain end (R₁-OH). Bottom: Block copolymers with isotactic-enriched (*it*) polyether moieties.



notably slower polymerization kinetics (Table 1, entries 9–12). To put this degree of selectivity into context, the observed bias for isotactic placement of PO by Al-porphyrin complexes is $m = 69\%$ at $20\text{ }^\circ\text{C}$.³ In contrast, the bimetallic catalysts reported by Coates are far superior in this regard ($mm > 99\%$, $0\text{ }^\circ\text{C}$).⁸

Control experiments employing the racemic mixture of **1** (*rac*-**1**) as well as **3** and **4** provided further insight. While *de facto* atactic PPO was observed by employing both the biphenyl derivative **3** and its linear congener **4** (Table 1), m remained unchanged by the switch from **1** to *rac*-**1** ($m = 82\%$ and 80% , respectively at $-36\text{ }^\circ\text{C}$, see Table S1† for further examples). This is intriguing from the perspective of practical application since using racemic mixtures may simplify future synthetic schemes for diborane preparation. Moreover, the overall monomer consumption is faster and expectedly identical for both PO enantiomers (Fig. S15†). The underlying reason for this behavior is most likely the strong association between the propagating polyether chain end (which is a secondary alkoxide) and borane functionality; very frequent chain exchange between diboranes seems unlikely in view of these results. The loss in selectivity observed when using biphenyl-based **3** could be attributed to its lower rotational barrier along the chirality axis and the higher flexibility regarding the phenyl–phenyl dihedral angle. Nonetheless, this compound may be a powerful co-catalyst if atactic polyether architectures are required (65% conversion after 30 minutes at 0.2 mol% diborane loading, entry 13).

In a next step, further epoxide monomers were screened, including 1-butylene oxide (BO), allyl glycidyl ether (AGE) and styrene oxide (SO). While SO could not be polymerized successfully, BO and AGE were polymerized to produce well-controlled polyethers with molar masses of 3000–31 000 g mol⁻¹. Stereoselectivity in general was comparable to that observed for PO ($m = 85\%$ (BO) and 78% (AGE), respectively). Polymerizations using enantiopure BO revealed the same tendency as described above for PO, namely a preference of **1** for the (*S*)-enantiomer of the monomer (Fig. S17†). A summary of all polymerizations is provided (Tables S1–S4†).

The ensuing polyether homopolymers (PPO, PBO, PAGE) are predominantly amorphous (Fig. S24–S26†); only those with the highest m values ($>85\%$) display moderately defined melting points (PPO with T_m up to $45\text{ }^\circ\text{C}$, Fig. S23,† as compared to $67\text{ }^\circ\text{C}$ for perfectly isotactic material¹). TGA analyses of atactic and *it*-enriched PPO revealed comparable behavior (Fig. S27†).

However, even if the degree of isotacticity is not sufficient to provide semi-crystalline behavior, polymeric additives can profit from isotactic enrichment. For example, *it*-enriched block copolyether additives have a systematic effect on the viscosity and storage/loss moduli if they are employed in aqueous environment to form hydrogels. A perfectly isotactic, semi-crystalline congener, on the other hand, failed under identical conditions on account of solubility issues.^{12c}

A further aspect of particular relevance for additives technology is the incorporation of *it*-enriched polyether moieties in more complex architectures, especially in conjunction with polyester blocks. The latter can so far only be included in a polyether-first approach, which means the polyester block is

grown on a (typically atactic) polyether macroinitiator. The reverse (polyester-first) is not readily possible since the polyester is susceptible to degradation under the reaction conditions used for epoxide conversion, including the conventional KOH-mediated polymerization but also organocatalytic- and metal-catalyzed polymerizations. To the best knowledge of the authors, this is also true for the previously reported iso- or enantioselective metal-based approaches for epoxide polymerization.¹ In sharp contrast, pronounced functional group tolerance regarding ester moieties should be inherent to borane co-catalysis, as was impressively demonstrated using Et₃B,²⁴ raising the possibility that polyester-first strategies and related polymer architectures could also be achievable for the chiral diborane catalysts presented here.

To investigate this, commercial and custom-made polyester macroinitiators (polycaprolactone (PCL) and polylactide (PLA), Scheme 2) were subjected to the same polymerization procedure as described above. This resulted in the corresponding diblock copolymers PCL-*b*-(*it*)-PPO and PLA-*b*-(*it*)-PPO as well as triblock copolymers ((*it*)-PPO-*b*-PCL-*b*-(*it*)-PPO). Block formation was substantiated by ¹H DOSY NMR (Fig. S28–S32†) and GPC analysis (Fig. S34–S36†). Notably, the narrow molar mass distribution confirms that no substantial transesterification occurs, and indeed it is possible to stir commercial PCL for 24 h (THF) in the presence of NHO/1 without any observable change in the molar mass of the macroinitiator (Fig. S33†). Once PO is added, the catalyst becomes active and leads to growth of the *it*-enriched polyether block. Likewise, it was possible to use α,ω -dihydroxy PEG 8000 as a bifunctional macroinitiator, resulting in isotactic-enriched variants of the well-known *Reverse Pluronic*-type triblock copolyethers, (*it*)-PPO-*b*-PEG-*b*-(*it*)-PPO. The data for these block copolymers are summarized in Table S4.†

Conclusions

In summary, an organocatalytic, cooperative catalyst based on readily available chiral diboranes enables the preparation of isotactic enriched aliphatic polyethers. Notably, the resulting polyether moieties are well-defined up to high molar masses and can be incorporated in block copolymers, including “polyester-first”-based architectures. It is believed that these abilities will be especially valuable for polymer additives manufacturing. The BINOL-type diborane platform is amenable to a plethora of structural modifications, which are currently studied in our group regarding their impact on stereoselectivity.

Data availability

Experimental setups, procedures and additional data (kinetics, ¹³C NMR, thermal analysis, GPC data) are available in the ESI.†

Author contributions

Experiments were planned and conducted by Ayla Sirin-Sarişlan under the supervision of Stefan Naumann. Writing was done by Ayla Sirin-Sarişlan with review by Stefan Naumann.



Conflicts of interest

There are no conflicts to declare.

Acknowledgements

Dr Wolfgang Frey and Dr Dongren Wang (both University of Stuttgart) are gratefully acknowledged for single crystal X-ray structure analysis and MALDI-ToF MS measurements, respectively. S. N. gratefully acknowledges funding by the German Research Foundation (Deutsche Forschungsgemeinschaft, DFG, NA 1206/3-1).

Notes and references

- 1 M. I. Childers, J. M. Longo, N. J. van Zee, A. M. LaPointe and G. W. Coates, *Chem. Rev.*, 2014, **114**, 8129–8152.
- 2 M. E. Pruitt and J. M. Baggett, *US Pat.*, 2706181, 1955.
- 3 See for example: N. Takeda and S. Inoue, *Makromol. Chem.*, 1978, **179**, 1377–1381.
- 4 E. J. Vandenberg, *J. Polym. Sci.*, 1960, **47**, 486–489.
- 5 R. C. Ferrier, S. Pakhira, S. E. Palmon, C. G. Rodriguez, D. J. Goldfeld, O. O. Iyiola, M. Chwatko, J. L. Mendoza-Cortes and N. A. Lynd, *Macromolecules*, 2018, **51**, 1777–1786.
- 6 K. L. Peretti, H. Ajiro, C. T. Cohen, E. B. Lobkovsky and G. W. Coates, *J. Am. Chem. Soc.*, 2005, **127**, 11566–11567.
- 7 W. Hirahata, R. M. Thomas, E. B. Lobkovsky and G. W. Coates, *J. Am. Chem. Soc.*, 2008, **130**, 17658–17659.
- 8 R. M. Thomas, P. C. B. Widger, S. M. Ahmed, R. C. Jeske, W. Hirahata, E. B. Lobkovsky and G. W. Coates, *J. Am. Chem. Soc.*, 2010, **132**, 16520–16525.
- 9 S. M. Ahmed, A. Poater, M. I. Childers, P. C. B. Widger, A. M. LaPointe, E. B. Lobkovsky, G. W. Coates and L. Cavallo, *J. Am. Chem. Soc.*, 2013, **135**, 18901–18911.
- 10 As a possible exception, a reviewer has pointed out that commercially available Hydrin®-elastomers are most likely prepared under application of the Vandenberg catalyst which allows for high-molar mass copolyethers and a moderate isotacticity (albeit it is not clear to what degree the latter is decisive for product properties).
- 11 J. Herzberger, K. Niederer, H. Pohlitz, J. Seiwert, M. Worm, F. R. Wurm and H. Frey, *Chem. Rev.*, 2016, **116**, 2170–2243.
- 12 See for example: (a) W. Shi, A. J. McGrath, Y. Li, N. A. Lynd, C. J. Hawker, G. H. Fredrickson and E. J. Kramer, *Macromolecules*, 2015, **48**, 3069; (b) A. J. McGrath, W. Shi, C. G. Rodriguez, E. J. Kramer, C. J. Hawker and N. A. Lynd, *Polym. Chem.*, 2015, **6**, 1465–1473; (c) F. Markus, J. R. Bruckner and S. Naumann, *Macromol. Chem. Phys.*, 2020, **221**, 1900437.
- 13 N. E. Kamber, W. Jeong, R. M. Waymouth, R. C. Pratt, B. G. G. Lohmeijer and J. L. Hedrick, *Chem. Rev.*, 2007, **107**, 5813.
- 14 A. P. Dove, *ACS Macro Lett.*, 2012, **1**, 1409.
- 15 M. Fèvre, J. Pinaud, Y. Gnanou, J. Vignolle and D. Taton, *Chem. Soc. Rev.*, 2013, **42**, 2142.
- 16 Y. Xia and J. Zhao, *Polymer*, 2018, **143**, 343.
- 17 J. Raynaud, W. N. Ottou, Y. Gnanou and D. Taton, *Chem. Commun.*, 2010, **46**, 3203.
- 18 S. Naumann, A. W. Thomas and A. P. Dove, *Angew. Chem., Int. Ed.*, 2015, **54**, 9550.
- 19 D. Zhang, S. K. Boopathi, N. Hadjichristidis, Y. Gnanou and X. Feng, *J. Am. Chem. Soc.*, 2016, **138**, 11117.
- 20 S. K. Boopathi, N. Hadjichristidis, Y. Gnanou and X. Feng, *Nat. Commun.*, 2019, **10**, 293.
- 21 Y. Chen, J. Shen, S. Liu, J. Zhao, Y. Wang and G. Zhang, *Macromolecules*, 2018, **51**, 8286.
- 22 C.-J. Zhang, H.-Y. Duan, L.-F. Hu, C.-H. Zhang and X.-H. Zhang, *ChemSusChem*, 2018, **11**, 4209.
- 23 C. Vogler and S. Naumann, *RSC Adv.*, 2020, **10**, 43389.
- 24 S. Liu, T. Bai, K. Ni, Y. Chen, J. Zhao, J. Ling, X. Ye and G. Zhang, *Angew. Chem., Int. Ed.*, 2019, **58**, 15478.
- 25 M. L. McGraw and E. Y.-X. Chen, *Macromolecules*, 2020, **53**, 6102.
- 26 G.-W. Yang, Y.-Y. Zhang, R. Xie and G.-P. Wu, *Angew. Chem., Int. Ed.*, 2020, **59**, 16910.
- 27 G.-W. Yang, Y.-Y. Zhang and G.-P. Wu, *Acc. Chem. Res.*, 2021, **54**, 4434.
- 28 X. Wang, J. Hui, M. Shi, X. Kou, X. Li, R. Zhong and Z. Li, *ACS Catal.*, 2022, **12**, 8434.
- 29 Y. Liu and H. Du, *J. Am. Chem. Soc.*, 2013, **135**, 6810.
- 30 S. Wei and H. Du, *J. Am. Chem. Soc.*, 2014, **136**, 12261.
- 31 Z. Zhang and H. Du, *Angew. Chem., Int. Ed.*, 2015, **54**, 623.
- 32 S. Kronig, P. G. Jones and M. Tamm, *Eur. J. Inorg. Chem.*, 2013, **2013**, 2301.
- 33 S. Naumann, *Chem. Commun.*, 2019, **55**, 11658.

